



Published in final edited form as:

J Proteome Res. 2011 July 1; 10(7): 3212–3224. doi:10.1021/pr200244f.

Proteomic characterization of early changes induced by triiodothyronine in rat liver

Valeria Severino¹, Joseph Locker², Giovanna M. Ledda-Columbano³, Amedeo Columbano³, Augusto Parente^{1,†}, and Angela Chambery^{1,†,§}

¹ Department of Life Science, Second University of Naples, Via Vivaldi 43, I-81100 Caserta, Italy

² Department of Pathology, Albert Einstein College of Medicine, 1300 Morris Park Ave., Bronx, NY, 10461, USA

³ Department of Toxicology, Oncology and Molecular Pathology Unit, University of Cagliari, Via Porcell 4, I-09124 Cagliari, Italy

Abstract

High doses of T3 are mitogenic in liver, causing hyperplasia that has numerous differences from the compensatory regeneration induced by partial hepatectomy (PH). T3 binds to the thyroid hormone receptor (TR), which directly regulates transcription, while PH acts indirectly through signal transduction pathways. We therefore carried out proteomic analysis to compare early effects of the two treatments. Transcriptome analysis by DNA microarray also confirmed the observed proteomic changes demonstrated that they were caused by transcriptional regulation. Among the differentially expressed proteins, many are directly or indirectly involved in energy metabolism or the response to oxidative stress. Several enzymes of lipid metabolism (e.g., Acaa2, Acads, Hadh, and Echs1) were differentially regulated by T3. In addition, altered expression levels of several mitochondrial proteins (e.g. Hspa9, Atp5b, Cps1, Glud1, Aldh2, Ak2, Acads) demonstrated the known increase of mitochondrial biogenesis mediated by T3. The present results provide insights in changes in metabolic balance occurring following T3-stimulation and define a basis for dissecting the molecular pathways of hepatocyte hyperplasia.

Keywords

Triiodothyronine; proteomic profiling; hepatectomy; liver regeneration

INTRODUCTION

The liver carries out many essential body functions. It regulates numerous metabolic processes, and acts as the gateway for all chemical substances absorbed through the gastrointestinal tract. Despite its large metabolic load, the liver is almost quiescent in terms of cell proliferation, with very few hepatocytes (<0.01%) undergoing mitosis^{1–4}. This low cell turnover in healthy liver can be altered by toxic liver injury or surgical resection, which results in the sudden and massive proliferation of hepatocytes. Surgical removal of 2/3 of the liver (2/3 PH) represents the most widely used model for studying the molecular changes responsible for the re-entry of hepatocytes into the cell cycle^{5, 6}. Indeed, several studies of

§To whom correspondence should be addressed; Mailing address: Dipartimento di Scienze della Vita, Seconda Università di Napoli, Via Vivaldi 43, I-81100 Caserta, Italy, Phone: +39 0823 274535; Fax: +39 0823 274571., angela.chambery@unina2.it.

†Equal contribution as co-last author

liver regeneration following PH have characterised their associated gene expression patterns^{7–10}.

Although DNA microarray technology provides insight on genes expression changes associated with liver regeneration, it fails to detect changes that occur at the translational and post-translational levels. Furthermore, in human liver and yeast cells, mRNA and protein levels may correlate poorly^{11, 12}. Thus, proteomics, a complementary tool for assessing global changes in cellular protein expression, provides unique insight into cellular responses. Unfortunately, despite the numerous studies of the gene expression profiles associated with liver regeneration following PH, only a few pioneering works have characterized the corresponding proteomic expression patterns^{13–18}. These studies revealed that the early response to PH showed differential expression of proteins involved in biotransformation, carbohydrate metabolism, lipid metabolism, the respiratory chain and oxidation–phosphorylation^{13–18}. Proteins involved in mitochondrial energy metabolism are of particular interest since this process is impaired immediately after PH with overproduction of reactive oxygen species (ROS) and an increase in the mitochondrial GSSG/GSH ratio, along with decreases in the respiratory control index and the rate of the oxidative phosphorylation^{19, 20}. Furthermore, accumulation of Ca²⁺ in mitochondria is concomitant with oxidative stress. Despite these biochemical events, usually regarded as pro-apoptotic, neither release of cytochrome c nor appearance of apoptotic nuclei are observed. Thus, the changes in mitochondria apparently serve to maintain their structural and functional integrity.

Recent studies have identified an increasing number of primary mitogens—peroxisome proliferators (PP), halogenated hydrocarbons, retinoic acids (RA), and thyroid hormone (T3)—able to induce hepatocyte proliferation without causing liver injury, i.e., direct hyperplasia²¹. Among these agents, T3 is a physiological hormone that has considerable potential for therapy of liver injury²². Liver gene expression changes between hypothyroid and hyperthyroid status after T3 administration were previously investigated^{23–26}. Moreover, a microarray analysis of mitogenic effects of T3 on the rat liver were also performed on euthyroid rats within 3 hr after stimulation²⁷. Complex changes in the transcripts levels of enzymes involved in intermediary metabolism were observed revealing the key role of T3 in the regulation of these processes. Nevertheless, the proteomic changes caused by a mitogenic dose of T3 have not been compared to those of liver regeneration. We therefore investigated whether protein changes in the early phases of liver regeneration were similar to those that occurred during liver hyperplasia induced by T3^{28–30}. To this aim, the proteomic profiling of rat liver samples following hepatocyte proliferation induced by a mitogenic dose of T3 was performed shortly after treatment and compared to liver regeneration after PH. Moreover, to correlate changes in protein content with mRNA levels, transcriptome analysis by DNA microarray was coupled to proteomic analysis.

EXPERIMENTAL SECTION

Materials

Chemical reagents and TPCK-treated trypsin were obtained from Sigma (Milan, Italy). Immobilized pH gradient (IPG) buffers, IPG strips, and electrophoresis apparatus were purchased from Amersham-Biosciences (Milan, Italy). BioRad (Milan, Italy) was the source of electrophoresis reagents, including acrylamide, N,N'-methylenebisacrylamide, N,N,N',N' tetramethylethylenediamine, ammonium persulfate and sodium dodecylsulfate (SDS). All other reagents were of analytical grade.

Animals

Male Wistar rats (175–200 g) purchased from Charles River (Milano, Italy) were treated as previously described³¹. Briefly, the animals were provided with food and water *ad libitum* with a 12 h light/dark daily cycle and were acclimated for one week before the start of the experiment. Institutional Guidelines for the Care and Use of Laboratory Animals during the investigation were followed. Three rats were used for each condition. T3 (Sigma Chemical Co., St. Louis, Mo.) was administered intraperitoneally as a single mitogenic dose of 20 µg/100 g body weight³¹. Two-thirds PH was performed according to Higgins and Anderson⁵. Livers harvested without surgery (controls), or at 6 h after PH- and T3-treatment, were snap-frozen in liquid nitrogen and stored at –80° C until use.

Microarray analysis

Total mRNA was isolated from livers using the guanidium isothiocyanate method (TRIzol; Invitrogen, Carlsbad, CA), followed by precipitation with LiCl⁹. 20 µg total RNA was labelled with the Superscript Plus Direct cDNA Labelling System with Alexa Fluor aha-dUTP (Invitrogen). Labelled product was purified and concentrated with a Microcon YM-50 column (Millipore). Two-color hybridization was carried out with red-labelled experimental sample and green-labelled pooled normal rat liver. The labelled cDNAs were hybridized overnight at 50° C on aminosilane-coated Corning (Corning, NY) glass slides spotted with 33,000 selected oligonucleotide sequences (70-mer Operon mouse 3.0 series), which were printed by the Microarray Core Facility of Albert Einstein College of Medicine. The microarrays were scanned with a GenePix 4000A scanner (Axon, Burlingame, CA), and data were acquired through GenePix Pro 6.0 software (Molecular Devices, Sunnyvale, CA). Hybridization data were further normalized without background subtraction, using locally weighted linear regression (LOWESS) analysis via an in-house program. RNA was isolated from three to four livers in each experimental group, following treatment with T3 or partial hepatectomy, each hybridized to a separate array. The averaged datasets were then compiled in Microsoft Access for further analysis. The analysis in this paper focuses on 6 h treatment with T3, except for cell cycle regulators Cyclin D1 and E1, which were characterized from sequential studies of both treatments.

Sample preparation for two-dimensional electrophoresis

The frozen tissue samples were transferred into quartz mortars and manually grounded in liquid nitrogen. Equal amounts (300 mg) of powdered tissue (100 mg pooled from three biological replicates) were lysed with 0.5 ml lysis buffer (40 mM Tris-HCl containing 8.3 M urea, 2M thiourea, 2% CHAPS, 1% DTT, and 1 mM PMSF), sonicated, and ultracentrifuged at 20000·g for 15 min at 4° C. The supernatants were collected and protein concentration determined by the Bradford method, according to manufacturer's instructions (Biorad, Milan, Italy). Lysates were aliquoted and stored at –80 °C until use.

Two-dimensional electrophoresis

A total of 700 µg of proteins per gel was analyzed in duplicate by two-dimensional electrophoresis (2DE), according to previously reported procedure^{s32, 33}. Samples to be processed by isoelectrofocusing (IEF) were mixed with rehydration buffer (8 M urea, 0.5% CHAPS, 0.2% DTT, 0.5% IPG ampholytes and 0.002% bromophenol blue) to a final volume of 340 µl. The precast IPG strips (3–10 linear pH gradient, 18 cm long), used for the first dimension, were passively rehydrated and loaded with the sample at room temperature for 12 h under low-viscosity paraffin oil. IEF was then performed using an IPGphor isoelectric focusing cell, according to the following protocol: 500 V for 700 Vh, 1000 V for 1400 Vh, and 8000 V for 34500 Vh. Strips were then equilibrated twice for 15 min with gentle shaking in equilibration solution (6 M urea, 50 mM Tris-HCl buffer, 30% glycerol,

2% SDS, 0.002% bromophenol blue, and 1% DTT), to reduce disulfide bonds, in the first equilibration step, and 2.5% iodoacetamide, to alkylate thiols, in the second. Separation by protein molecular mass was performed in an Ettan DALTsix Electrophoresis Unit on homogeneous polyacrylamide gels (12% T, 1% C). The equilibrated strips were sealed to the top of the vertical gel with agarose solution (agarose 0.5% and 0.002% bromophenol blue dissolved in SDS/Tris running buffer) and electrophoresis was carried out at constant power (2.5 W/gel for 30 min followed by 100 W/gel for about 4 h and 30 min) and temperature (20 °C), until the blue dye reached the bottom of the gel. At the end of the electrophoresis, the gels were fixed in 50% methanol/ 10% acetic acid for 2 h, and the protein spots visualized by incubating overnight with colloidal Coomassie blue stain (2% phosphoric acid, 10% ammonium sulphate, 20% methanol, 0.1% Coomassie brilliant blue G-250), followed by three two-hours washes with deionised water.

Gel scanning and image analysis

Stained 2D gels were scanned and analysed to compare matching spots. Gels were scanned using a Molecular Dynamics densitometer, model 375–557 (Amersham Biosciences, Milan, Italy). Gel images were processed for spot detection, background subtraction, and matching, using Melanie Image Master 2D Platinum 7.04 software (GE Healthcare, Milan, Italy). For image analysis, the proteomic profile of control rat liver was used as reference pattern and all conditions (T3-induced and PH samples) were matched to the reference pattern. Briefly, relative intensity (RI= v_i/v_t) of each spot was calculated by dividing volume of the spot by the total volume of the detected spots on the gels, multiplied by the total area of all the spots. Spots were considered to be differentially expressed if they were either present in different amount or absent in comparison with the reference gel, and quantitatively different to corresponding controls when their normalized total volume values differed significantly ($P \leq 0.05$) based on ANOVA analysis. Expression intensity ratios of PH/control and T3-treated/control ≥ 1.5 and ≤ 0.5 were set as thresholds indicating significant change.

In-gel tryptic digestion

Selected protein spots by 2DE gel image analysis were excised from gels and destained by washing twice with 100 μ l of water, followed by a further washing step with 50% acetonitrile. The gel pieces were then dried in a SpeedVac Vacuum (Savant Instruments, Holbrook, NY) and rehydrated with 15 μ l of 50 mM ammonium bicarbonate, followed by the addition of 1 μ l of 70 ng/ml TPCK-treated bovine trypsin solution³³. Digestion was performed by incubation at 37 °C for 3 h. Further amounts of buffer solution without trypsin were added when necessary to keep the gel pieces wet during the digestion. Peptides were extracted in two steps by sequential addition of 1% trifluoroacetic acid (TFA) and then of 2% TFA/ 50% acetonitrile for 10 min in a sonication bath. The combined supernatants were concentrated in the SpeedVac Vacuum for mass spectrometry (MS) analysis^{32, 33}.

Protein identification by MALDI-TOF mass spectrometry

Protein identification by matrix-assisted laser desorption/ionization time-of-flight mass spectrometry (MALDI-TOF MS) was performed according to Severino et al.³². Briefly, after *in situ* tryptic digestion, aliquots of tryptic peptides (1 μ l) were mixed with an equal volume of saturated α -cyano-4-hydroxycinnamic acid matrix solution (10 mg/ml in acetonitrile 50% in water) and spotted onto a MALDI-TOF target plate. The droplet was dried at room temperature. Once the liquid was completely evaporated, the sample was loaded into the mass spectrometer and analyzed. Peptide spectra were collected in positive ion reflectron mode on a MALDI-TOF micro MX (Waters Co., Manchester, UK), equipped with a pulsed nitrogen laser ($\lambda=337$ nm). The instrument source voltage was set to 12 kV. The pulse voltage was optimized at 1999 V, the detector and reflectron voltages were set to 5200 V and 2350 V, respectively. Measurements were performed in the mass range m/z

850–3000 with a suppression mass gate set to m/z 500 to prevent detector saturation from matrix cluster peaks and an extraction delay of 600 ns. The instrument was externally calibrated using a tryptic alcohol dehydrogenase digest (Waters, Milford, MA USA) as standard. A mass accuracy near to the nominal (50 ppm) was achieved for each standard. The protonated monoisotopic mass of ACTH peptide (m/z 2465.199) was used as internal lock mass to further improve the peptide mass accuracy. All spectra were processed and analyzed using MassLynx 4.1 software (Waters, Milford, MA USA). The obtained spectra were used to identify proteins by searching a *Rattus norvegicus* species-specific Swiss-Prot database (release 57.0, number of entries 7314) by using Protein Lynx Global Server 2.3 software (Waters Co., Manchester, UK). The following searching parameters were used: trypsin specificity for protein cleavage; mass tolerance 100 ppm; allowed number of missed cleavage sites up to 1; cysteine residues modified as carbamidomethyl-cys; minimum number of matched peptides 3.

Pathway analysis

The pathway analysis for differentially identified proteins was performed using Ingenuity Pathways Analysis (IPA) software, version 6.3 (Ingenuity Systems, <http://www.ingenuity.com>). The lists of differentially expressed proteins were imported into the IPA platform for batch analysis and identification of the canonical pathways that differ between the analysed conditions was performed as previously reported^{32, 34}.

RESULTS

Both high dose T3 treatment (200 $\mu\text{g}/\text{kg}$) and PH induce DNA synthesis and cell division in the rat. Both high dose T3 treatment (200 $\mu\text{g}/\text{kg}$) and PH induce DNA synthesis and cell division in the rat. Microarray analysis of mRNA for Cyclins D1 (CcnD1) and E1 (CcnE1) highlights differences between the two proliferative responses (Figure 1). In both cases, the peak of cyclin E1 precedes the G1-S interface, and occurs 6 h after T3 treatment and 12 h after PH. Being a direct ligand of a nuclear receptor transcription factor, T3 exerts a rapid effect on gene expression, likely explaining the more rapid increase observed in T3 treated rats. As expected, PH induces a stronger proliferative response than T3, with 1.8- and 3.2-fold greater peak values of CcnD1 and CcnE1, respectively. Although the PH and T3 responses at 6 h are not synchronous at cell cycle level, we focused on this time point since it precedes the restriction point in G1 phase¹⁴ and the induction of direct T3 target genes is strong. At an almost identical time point (7 h) after PH, prominent expression changes at protein level were previously observed¹⁴.

Total liver proteins were extracted from control, PH and T3-treated (T3) samples and separated by 2D-PAGE using IPG strips with a linear 3–10 pH gradient. A representative 2D-PAGE map obtained from control sample is shown in Figure 2A, while those derived from PH- and T3-treated samples at 6 h are shown in Figure 3A and B, respectively. For reliable analysis of protein expression, 2D gel maps of each sample were performed and analyzed in duplicate. These showed high correlation coefficients, indicating a high reproducibility. A representative scatter plot for a control sample is shown in Figure 2B, demonstrating a correlation coefficient of 0.98. Similar plots were obtained for PH and T3 samples with correlation coefficients of 0.99 and 0.85, respectively. For the control set, 310 ± 28 spots were detected, while for the PH and T3 samples 252 ± 2 and 322 ± 23 spots were detected, respectively. Both PH and T3 samples were compared with the control sample for spot matching. A high number of matched spots was detected for both PH (192 spots, coverage 72%) and T3 (186 spots, coverage 58%). A high matching percentage (67%) was revealed when T3-treated rat liver samples were compared to the PH model. An overview of the differentially expressed proteins was obtained by comparing the 2D gels of the two analysed conditions to the control map. Gel image analysis yielded lists of differentially

expressed proteins that showed qualitative or quantitative differences between the two treatments. In particular, 84 spots were quantitatively differentially expressed (ratio ≥ 1.5 and ≤ 0.5) in at least one condition (Table 1). In addition, 15 spots were uniquely revealed under a given condition (Table 2), most corresponding to differentially expressed isoforms of proteins reported in Table 1.

We then used an independent approach to confirm the expression changes of a subset of differentially regulated proteins (Table 3). To this aim, microarray analysis determined the mRNA levels of the proteins listed in Table 1 following T3 stimulation. Simple linear regression ($p < 0.0001$, $R^2 = 0.285$; not illustrated) showed strong correlation of mRNA and protein levels, with only a single outlier, argininosuccinate synthase (Ass1). There were two complexities in this correlation. First was the presence of isoforms. Each isoform spot, and the sum of all isoforms for a particular protein, were compared to mRNA levels (not illustrated). The principal spots gave an excellent correlation ($p = 0.0002$), but the levels of many isoforms were much higher and did not correlate with mRNA levels. This may indicate that many of the isoforms resulted from post-transcriptional modifications that protected the protein from normal turnover. Second, the appearance of the distribution suggested two populations with different relationships between the RNA and protein expression levels (Figure 4). Further analysis showed that the values could be fitted to two parallel regression lines, with different y intercepts (population 1, $p < 0.0001$, $R^2 = 0.65$; population 2, $p < 0.0001$, $R^2 = 0.68$). These lines suggest classes of mRNA with different translation efficiencies, or proteins with different turnover rates. Alternatively, they might simply reflect a technical difference, since Coomassie detection of individual proteins may vary. Despite these complexities, the mRNA analysis independently confirmed the protein quantifications, and further demonstrated that both increases and decreases in protein abundance resulted from transcriptional regulation, the expected mechanism for regulation by a nuclear receptor transcription factor. The analysis also demonstrates that by 6 hr after treatment, the synthesis and turnover rates of mRNA and protein have both equilibrated to a point where global correlations can be observed.

A classification of the differentially expressed proteins was performed according to the canonical pathways in which they are involved by using Ingenuity Pathways Analysis (IPA) software. These pathways mainly include proteins related to amino acid, lipid and carbohydrate metabolism, oxidative stress response, energy production, cell-to-cell signalling, and cell interactions. In all networks, the highest number of identified proteins was cytosolic, including the organellar proteins. Additional cluster analysis of the differentially expressed proteins was also performed on the basis of their molecular functions. The greatest number of identified proteins in both conditions were enzymes, including kinases, e.g., adenylate kinase 2 (Ak2, spot 36) and phosphoglycerate kinase 1 (Pkg11, spot 54). Six transcription regulators, e.g., calreticulin (Calr, spot 33), nucleophosmin 1 and alpha enolase 1 (Eno1, spots from 8 to 8c), were also differentially expressed in PH and T3 samples.

In addition, many molecular chaperones and folding catalysts were found differentially expressed following PH and T3 treatment (Supplementary Figure 1, Supporting Information). Among proteins involved in protein folding, peptidylprolyl cis-trans isomerase (Ppia, cyclophilin A, spots 65 and 65a) was found slightly up-regulated in T3-treated rats, showing also the presence of a second acidic isoform (Supplementary Figure 1E) with respect to control and PH samples. Members of the heat shock protein 70 family (HSPs) were differentially regulated, including 78 kDa glucose regulated protein (Hspa5 spot 1, Supplementary Figure 1A), stress 70 protein mitochondrial (Hspa9 spots from 3 to 3b Supplementary Figure 1B), heat shock related 70 kDa (Hspa2 spot 41, Supplementary

Figure 1C) and heat shock 70 kDa (Hspa1b spot 47, Supplementary Figure 1D). For several HSPs, a common response was revealed for both PH and T3 treatment.

In addition, proteins involved in the oxidative stress response were differentially expressed (Supplementary Figure 2, Supporting Information), such as the superoxide dismutase 1 (Sod1, spots 26 and 26a). The main Sod1 isoform showed increased expression levels in both conditions. For the liver arginase 1 (Arg1, spots 28 and 28a), involved in the urea cycle and in nitric oxide response, the increasing of a strong acidic isoform was observed in both PH and T3 stimulated samples (Supplementary Figure 2H).

Many differentially expressed proteins were involved in energy metabolism (Supplementary Figure 3, Supporting Information), in particular, enzymes involved in fatty acid beta-oxidation. These included enoyl CoA hydratase (Echs1, spots 19 and 19a), hydroxyacyl-coenzyme A dehydrogenase (Hadh, spot 69), 3-ketoacyl CoA thiolase (Acaa2, spots 10 and 10a), and acyl CoA dehydrogenase (Acads, spots 38 and 38a). To further investigate the lipid metabolism response following T3 treatment, we used microarrays to detect expression changes of additional lipid regulators that were below the threshold of proteomic detection (Table 4). T3 stimulated expression of several enzymes involved in lipolysis including patatin-like phospholipase domain-containing protein 2 (Pnpla2), monoglyceride lipase (Mgll), and lysophospholipase 2 (Lypla2). Genes coding for the “carnitine shuttle” enzymes—carnitine-acylcarnitine translocase (Crat) and carnitine palmitoyltransferase (Cpt1a)—were also up-regulated following T3 stimulation.

Lipid metabolism is closely connected to the metabolism of carbohydrates that may be converted to fats. Therefore it is not surprising that proteomic analysis also showed significant differences of several metabolic enzymes (e.g. fructose 1,6 bisphosphatase) between PH and T3 samples (see discussion). Significantly enriched categories for differentially expressed proteins upon T3 stimulation were related to biological functions and tissue related pathologies using IPA software (Figure 5). The significantly enriched categories under biological function of differentially expressed proteins revealed that most of them were involved in oxidative stress and fatty acid metabolism (Figure 5A). In particular, a significant number of proteins was involved in the oxidative stress response mediated by Nrf2. This transcription factor is a crucial player in the defence against oxidative stress whose role in liver regeneration has been recently proposed based on the regulation of the ROS-mediated insulin/IGF-1 resistance³⁵. As expected, with regard the biological effects of treatment, the largest category was related to liver hyperplasia/hyperproliferation for both PH and T3 stimulated samples (Figure 5B).

To better understand the mutual interactions of differentially identified proteins, network maps were constructed using the in silico IPA software. The pathways obtained for PH are reported in Supplementary Figure 4, Supporting Information. The first two pathways converged on NFκB-p38MAPK and TNFα-INFγ networks with twenty-four and thirteen proteins, respectively. It is well known that NFκB is activated by TNFα after PH, leading to the priming of hepatocytes and enhancing their sensitivity to mitogens (e.g. HGF, EGF, TGFα)³⁶. In addition, two additional pathways—converging on MYC-ERK-AKT and GLUT4 (SLC2A4)-Hepatocyte nuclear factor 4α (HNF4A) signalling—were identified in PH (Supplementary Figure 5, Supporting Information). Both pathways are known to be involved in a variety of functions related with apoptosis, proliferation, and cell-cycle progression³⁷. In particular, HNF4A, a transcription factor of the nuclear hormone receptor superfamily, defines the expression of liver-specific genes encoding apolipoproteins, serum factors, cytochrome P-450 isoforms and proteins involved in the metabolism of glucose, fatty acids, and amino acids essential for hepatocyte differentiation and liver development³⁶. The differentially expressed proteins after T3 stimulation converged on pathways involving

similar core molecules, i.e., NFkB-p38MAPK and GLUT4-Leptin networks, (Supplementary Figure 6, Supporting Information). Indeed, twenty-four proteins were involved in the NFkB-p38MAPK pathway, while seventeen proteins were mapped on the GLUT4-Leptin network. It should be noted that although the resulting pathways are very similar, the occurrence of common activation signalling cascade cannot be inferred on the basis of present data. Indeed, several differentially expressed proteins among T3 and PH conditions could have a different effects, (i.e., activation or inhibition), on the pathways. These mechanisms, however, are highly complex and their proper interpretation would require further investigation which lies outside the scope of the present study.

DISCUSSION

The finding that many hepatomitogens are ligands of nuclear receptors led us to hypothesize that signal transduction pathways in hyperplasia were different from those of in liver regeneration, since the latter are mediated by classical membrane-receptors^{21, 31}. Among hepatomitogens, T3 is of particular interest, since its administration causes a rapid regression of carcinogen-induced hepatic nodules, and reduces the incidence of hepatocellular carcinoma and lung metastasis³⁸. Thus, precise knowledge of the mechanisms causing the mitogenic effect of T3 could lead to therapies for liver cancer, as well as therapies that stimulate liver repopulation after injury or transplantation.

The present work focuses on early molecular events occurring after treatment with T3, to investigate specific changes of gene and protein expression patterns. The differentially expressed proteins were involved in pathways related to energy metabolism, carbohydrates, lipids, and amino acids (Figure 6). In addition, pathways of oxidative stress, xenobiotic detoxification, and urea metabolism were also altered after T3 treatment.

As a vital organ, the liver must maintain metabolic homeostasis and energy supply during the regenerative process. Thus it is not surprising that several proteins associated with glycolysis/gluconeogenesis pathways were differentially expressed between PH and T3 treatment. One is fructose 1,6 biphosphatase, a key enzyme involved in gluconeogenesis. This enzyme was slightly down-regulated in PH but up-regulated after T3 treatment. Gluconeogenesis, together with glycogen breakdown, contributes to both to glucose homeostasis, and synthetic pathways^{39, 40}. Similarly, some glycolytic enzymes—e.g., fructose biphosphate/ aldolase B (Fbp1) and glyceraldehyde-3-phosphate dehydrogenase (Gapdh)—were down-regulated in both conditions. Despite the loss of two thirds of its functional mass, the liver is capable of stabilizing the blood glucose by increasing gluconeogenesis and glycogenolysis. It also shifts energy substrate utilization from glucose to free fatty acids (FFA). Intracellular energy demand increases during the early PH phases when glycolysis is preferentially utilized for ATP supply by the surviving hepatocytes. Subsequently FFA are the main energy substrate⁴¹. Accordingly, induction of enzymes isoforms involved in lipid metabolism (e.g., Acaa2, Acads, Hadh, and Echs1) were differentially expressed upon T3 stimulation. Among these, acyl-CoA dehydrogenase (Acads) is involved in the beta-oxidation of short chain fatty acids. This finding is of particular interest as it has been reported that liver regeneration process is impaired when fatty acid oxidation is inhibited by inhibitors of beta-oxidation⁴².

Beyond their roles in energy storage and as membrane constituents, fatty acids are also bioactive molecules that regulate a multitude of physiological processes. Thus, the increased β -oxidation might change intracellular signalling by peroxisome proliferator-activated receptors (PPAR)⁴³. PPAR are the major regulators of lipid and fatty acid metabolism and regulate transport, oxidation, storage, and synthesis. Furthermore, responses mediated by several other transcription factors are regulated by fatty acid regulation, including sterol

regulatory element binding protein-1c (SREBP1c), hepatic nuclear factor 4 (HNF4), the retinoid X receptor (RXR), and the liver X receptor (LXR)^{44–46}.

Several lines of evidence suggest that fatty acids generated from intracellular triacylglycerol hydrolysis may have important roles in signalling by PPAR⁴³, and our data show that signalling by TR also affects these pathways. In this framework, lipolysis is an important metabolic pathway controlling energy homeostasis through degradation of triglycerides stored in lipid droplets and release of fatty acids. Lipid droplets include a neutral lipid core composed largely of triglycerides, surrounded by a phospholipid monolayer and coated with surface proteins. Triglyceride hydrolysis represents a significant source of intracellular fatty acids. T3 stimulates enzymes that regulate these droplets, including the adipose differentiation related protein (Adfp) and patatin-like phospholipase domain-containing protein 2 (Pnpla2; also known as adipose triglyceride lipase, ATGL). Pnpla2 catalyzes the initial hydrolysis of triglycerides into diglycerides while Adfp is a major component of the lipid droplet surface. T3 also stimulates up-regulation of the apolipoprotein A-IV, a major lipid-transporter. Two genes coding for “carnitine shuttle” enzymes (carnitine-acylcarnitine translocase, carnitine palmitoyltransferase), used by the cell to facilitate the import of hydrophobic long-chain fatty acids from the cytosol into the mitochondrial matrix, were also up-regulated following T3 stimulation.

Other metabolic pathways play a key role in the regulation of events that are necessary for liver regeneration, including the transsulfuration pathway—that utilizes methionine for GSH synthesis—is particularly active in the liver⁴⁷. This pathway also links to metabolism of S-adenosine methionine (SAM) a methyl donor and a key metabolite that regulates hepatocyte growth, death, and differentiation^{48–51}. Several differences between PH and T3 treatment related to arginine metabolism. Arginine functions as a precursor for the synthesis not only of proteins, but also of nitric oxide, urea, polyamines, proline, glutamate and creatine^{52,53}. Two isoforms of arginase 1 (Arg1) were identified in both T3 and PH samples. Although an overall up-regulation was revealed for the arginase isoforms, their regulation levels were slightly different for T3 and PH samples. Similarly, two other enzymes involved in the arginine metabolism—carbamoyl-P synthase (Cps1) and argininosuccinate synthase (Ass1)—showed different regulation after T3 and PH treatment. In particular, Ass1, which catalyzes the synthesis of argininosuccinate from citrulline and aspartate, is strongly up-regulated by T3 but down-regulated following hepatectomy. Taken together these results suggest differences in arginine metabolism that can be related to the production of nitric oxide, a well known inducer of oxidative stress. Moreover, treatment with T3 has been demonstrated to induce oxidative stress in rat liver⁵⁴.

Intracellular antioxidant enzyme activities, and exogenously administered antioxidants, can modulate liver proliferation^{20, 55,42}. Oxidative stress can also lead to damage of thiols, lipids, proteins, and nucleic acids⁵⁶. Thus, it is not surprising that several differentially expressed proteins induced by both PH and T3 were modulators of oxidative stress. Among these cellular protective enzymes, glutathione S-transferase protects against oxidant toxicity and contributes to the regulation of stress-mediated apoptosis⁵⁷. Two other differentially expressed proteins involved in the oxidative stress response are superoxide dismutase (Sod1) and peroxiredoxin 1 (Pdx1). The latter, involved in the detoxification of hydrogen peroxide, was strongly and selectively up-regulated after T3 treatment.

CONCLUSIONS

This study represents the first attempt to identify, by a proteomic approach, differences between the hepatic proliferative responses induced by T3 and liver regeneration. Microarray analysis of mRNA confirmed the proteomic findings, and demonstrated that the

changes in protein levels were caused by transcriptional regulation. A more comprehensive transcriptomic characterization of the T3-induced mRNA expression is in progress but outside of the scope of the present study. We mapped a highly orchestrated series of molecular events that can derive and/or influence cellular proliferation. Several expressed proteins showed similar effects after both PH and T3 treatment. Those showing differential effects of T3 treatment were mainly metabolic enzymes, and this paper provides the first proteomic characterization of these metabolic changes. The differential regulation of transcripts and proteins involved in lipid and energy metabolism following T3 stimulation deserves further investigation since it is known that changes in cellular energy metabolism are associated with liver regeneration. Cell proliferation and metabolic regulation must occur in a synchronous manner as recently highlighted in cancer model systems⁵⁸. The metabolic changes related to regeneration and hyperplasia are therefore of fundamental importance for understanding the coordination of DNA synthesis and mitosis that drive liver cell proliferation. The regulation of metabolic pathways often occurs by covalent modification of key hepatic enzymes (e.g., phosphorylation/dephosphorylation or acetylation/deacetylation). Although the deeper characterization of post-translational modification of metabolic enzymes is beyond the scope of this work, the occurrence of multiple isoforms for several enzymes suggests the occurrence of enzyme regulation at the post-translational level. This study has demonstrated proteomic changes that distinguish T3 treatment from liver regeneration. Further studies that characterize the specific modifications of these proteins will provide unique insight into the mechanism by which T3 induces hepatocyte proliferation.

Supplementary Material

Refer to Web version on PubMed Central for supplementary material.

Acknowledgments

This study was supported by funds from the Second University of Naples, AIRC (Grant IG-5925), Italy; and NIH grant CA104292, USA.

References

1. Starzl TE, Porter KA, Francavilla JA, Benichou J, Putnam CW. A hundred years of the hepatotrophic controversy. *Ciba Found Symp.* 1977; 55:111–29. [PubMed: 207494]
2. Fausto N, Webber EM. Control of liver growth. *Crit Rev Eukaryot Gene Expr.* 1993; 3 (2):117–35. [PubMed: 8324292]
3. Diehl AM, Rai R. Review: regulation of liver regeneration by pro-inflammatory cytokines. *J Gastroenterol Hepatol.* 1996; 11 (5):466–70. [PubMed: 8743919]
4. Michalopoulos GK, DeFrances MC. Liver regeneration. *Science.* 1997; 276 (5309):60–6. [PubMed: 9082986]
5. Higgins AR. Experimental pathology of the liver. I. Restoration of the liver of the white rat following surgical removal. *Archives of Pathology and Laboratory Medicine.* 1931; (12):186–206.
6. Palmes D, Spiegel HU. Animal models of liver regeneration. *Biomaterials.* 2004; 25 (9):1601–11. [PubMed: 14697862]
7. White P, Brestelli JE, Kaestner KH, Greenbaum LE. Identification of transcriptional networks during liver regeneration. *J Biol Chem.* 2005; 280 (5):3715–22. [PubMed: 15546871]
8. Fukuhara Y, Hirasawa A, Li XK, Kawasaki M, Fujino M, Funeshima N, Katsuma S, Shiojima S, Yamada M, Okuyama T, Suzuki S, Tsujimoto G. Gene expression profile in the regenerating rat liver after partial hepatectomy. *J Hepatol.* 2003; 38 (6):784–92. [PubMed: 12763372]
9. Locker J, Tian J, Carver R, Concas D, Cossu C, Ledda-Columbano GM, Columbano A. A common set of immediate-early response genes in liver regeneration and hyperplasia. *Hepatology.* 2003; 38 (2):314–25. [PubMed: 12883475]

10. Cressman DE, Greenbaum LE, DeAngelis RA, Ciliberto G, Furth EE, Poli V, Taub R. Liver failure and defective hepatocyte regeneration in interleukin-6-deficient mice. *Science*. 1996; 274 (5291): 1379–83. [PubMed: 8910279]
11. Gygi SP, Rochon Y, Franza BR, Aebersold R. Correlation between protein and mRNA abundance in yeast. *Mol Cell Biol*. 1999; 19 (3):1720–30. [PubMed: 10022859]
12. Anderson L, Seilhamer J. A comparison of selected mRNA and protein abundances in human liver. *Electrophoresis*. 1997; 18 (3–4):533–7. [PubMed: 9150937]
13. Cao H, Yu J, Xu W, Jia X, Yang J, Pan Q, Zhang Q, Sheng G, Li J, Pan X, Wang Y, Li L. Proteomic analysis of regenerating mouse liver following 50% partial hepatectomy. *Proteome Sci*. 2009; 7:48. [PubMed: 20040084]
14. Guo F, Nian H, Zhang H, Huang L, Tang Y, Xiao X, He D. Proteomic analysis of the transition from quiescent to proliferating stages in rat liver hepatectomy model. *Proteomics*. 2006; 6 (10): 3075–86. [PubMed: 16619303]
15. Hsieh HC, Chen YT, Li JM, Chou TY, Chang MF, Huang SC, Tseng TL, Liu CC, Chen SF. Protein profilings in mouse liver regeneration after partial hepatectomy using iTRAQ technology. *J Proteome Res*. 2009; 8 (2):1004–13. [PubMed: 19099420]
16. Strey CW, Winters MS, Markiewski MM, Lambris JD. Partial hepatectomy induced liver proteome changes in mice. *Proteomics*. 2005; 5 (1):318–25. [PubMed: 15602770]
17. Sun Q, Miao M, Jia X, Guo W, Wang L, Yao Z, Liu C, Jiao B. Subproteomic analysis of the mitochondrial proteins in rats 24 h after partial hepatectomy. *J Cell Biochem*. 2008; 105 (1):176–84. [PubMed: 18523981]
18. Sun Y, Deng X, Li W, Yan Y, Wei H, Jiang Y, He F. Liver proteome analysis of adaptive response in rat immediately after partial hepatectomy. *Proteomics*. 2007; 7 (23):4398–407. [PubMed: 17979177]
19. Guerrieri F, Pellicchia G, Lopriore B, Papa S, Esterina Liquori G, Ferri D, Moro L, Marra E, Greco M. Changes in ultrastructure and the occurrence of permeability transition in mitochondria during rat liver regeneration. *Eur J Biochem*. 2002; 269 (13):3304–12. [PubMed: 12084072]
20. Lee FY, Li Y, Zhu H, Yang S, Lin HZ, Trush M, Diehl AM. Tumor necrosis factor increases mitochondrial oxidant production and induces expression of uncoupling protein-2 in the regenerating mice [correction of rat] liver. *Hepatology*. 1999; 29 (3):677–87. [PubMed: 10051468]
21. Columbano A, Shinozuka H. Liver regeneration versus direct hyperplasia. *Faseb J*. 1996; 10 (10): 1118–28. [PubMed: 8751714]
22. Columbano A, Simbula M, Pibiri M, Perra A, Deidda M, Locker J, Pisanu A, Uccheddu A, Ledda-Columbano GM. Triiodothyronine stimulates hepatocyte proliferation in two models of impaired liver regeneration. *Cell Prolif*. 2008; 41 (3):521–31. [PubMed: 18422700]
23. Weitzel JM, Hamann S, Jauk M, Lacey M, Filbry A, Radtke C, Iwen KA, Kutz S, Harneit A, Lizardi PM, Seitz HJ. Hepatic gene expression patterns in thyroid hormone-treated hypothyroid rats. *J Mol Endocrinol*. 2003; 31 (2):291–303. [PubMed: 14519097]
24. Weitzel JM, Radtke C, Seitz HJ. Two thyroid hormone-mediated gene expression patterns in vivo identified by cDNA expression arrays in rat. *Nucleic Acids Res*. 2001; 29 (24):5148–55. [PubMed: 11812848]
25. Feng X, Jiang Y, Meltzer P, Yen PM. Thyroid hormone regulation of hepatic genes in vivo detected by complementary DNA microarray. *Mol Endocrinol*. 2000; 14 (7):947–55. [PubMed: 10894146]
26. Flores-Morales A, Gullberg H, Fernandez L, Stahlberg N, Lee NH, Vennstrom B, Norstedt G. Patterns of liver gene expression governed by TRbeta. *Mol Endocrinol*. 2002; 16 (6):1257–68. [PubMed: 12040013]
27. Bungay A, Selden C, Brown D, Malik R, Hubank M, Hodgson H. Microarray analysis of mitogenic effects of T3 on the rat liver. *J Gastroenterol Hepatol*. 2008; 23 (12):1926–33. [PubMed: 18717759]
28. Francavilla A, Carr BI, Azzarone A, Polimeno L, Wang Z, Van Thiel DH, Subbotin V, Prelich JG, Starzl TE. Hepatocyte proliferation and gene expression induced by triiodothyronine in vivo and in vitro. *Hepatology*. 1994; 20 (5):1237–41. [PubMed: 7927257]

29. Malik R, Habib M, Tootle R, Hodgson H. Exogenous thyroid hormone induces liver enlargement, whilst maintaining regenerative potential--a study relevant to donor preconditioning. *Am J Transplant.* 2005; 5 (8):1801–7. [PubMed: 15996226]
30. Kowalik MA, Perra A, Pibiri M, Cocco MT, Samarut J, Plateroti M, Ledda-Columbano GM, Columbano A. TRbeta is the critical thyroid hormone receptor isoform in T3-induced proliferation of hepatocytes and pancreatic acinar cells. *J Hepatol.* 2010; 53 (4):686–92. [PubMed: 20638743]
31. Pibiri M, Ledda-Columbano GM, Cossu C, Simbula G, Menegazzi M, Shinozuka H, Columbano A. Cyclin D1 is an early target in hepatocyte proliferation induced by thyroid hormone (T3). *Faseb J.* 2001; 15 (6):1006–13. [PubMed: 11292661]
32. Severino V, Chambery A, Vitiello M, Cantisani M, Galdiero S, Galdiero M, Malorni L, Di Maro A, Parente A. Proteomic analysis of human U937 cell line activation mediated by Haemophilus influenzae type b P2 porin and its surface-exposed loop 7. *J Proteome Res.* 2010; 9 (2):1050–62. [PubMed: 20043682]
33. Chambery A, Farina A, Di Maro A, Rossi M, Abbondanza C, Moncharmont B, Malorni L, Cacace G, Pocsfalvi G, Malorni A, Parente A. Proteomic analysis of MCF-7 cell lines expressing the zinc-finger or the proline-rich domain of retinoblastoma-interacting-zinc-finger protein. *J Proteome Res.* 2006; 5 (5):1176–85. [PubMed: 16674107]
34. Mendelsohn BA, Malone JP, Townsend R, Gitlin J. Proteomic analysis of anoxia tolerance in the developing zebrafish embryo. *Comparative Biochemistry and Physiology, Part D.* 2009; 4 (1):21–31.
35. Beyer TA, Xu W, Teupser D, auf dem Keller U, Bugnon P, Hildt E, Thiery J, Kan YW, Werner S. Impaired liver regeneration in Nrf2 knockout mice: role of ROS-mediated insulin/IGF-1 resistance. *Embo J.* 2008; 27 (1):212–23. [PubMed: 18059474]
36. Taub R. Liver regeneration 4: transcriptional control of liver regeneration. *Faseb J.* 1996; 10 (4): 413–27. [PubMed: 8647340]
37. Wierstra I, Alves J. The c-myc promoter: still MysterY and challenge. *Adv Cancer Res.* 2008; 99:113–333. [PubMed: 18037408]
38. Ledda-Columbano GM, Perra A, Loi R, Shinozuka H, Columbano A. Cell proliferation induced by triiodothyronine in rat liver is associated with nodule regression and reduction of hepatocellular carcinomas. *Cancer Res.* 2000; 60 (3):603–9. [PubMed: 10676643]
39. Rosa JL, Bartrons R, Tauler A. Gene expression of regulatory enzymes of glycolysis/ gluconeogenesis in regenerating rat liver. *Biochem J.* 1992; 287 (Pt 1):113–6. [PubMed: 1329724]
40. Haber BA, Chin S, Chuang E, Buikhuisen W, Naji A, Taub R. High levels of glucose-6-phosphatase gene and protein expression reflect an adaptive response in proliferating liver and diabetes. *J Clin Invest.* 1995; 95 (2):832–41. [PubMed: 7860767]
41. Lai HS, Chen WJ, Chen KM. Energy substrate for liver regeneration after partial hepatectomy in rats: effects of glucose vs fat. *JPN J Parenter Enteral Nutr.* 1992; 16 (2):152–6. [PubMed: 1556811]
42. Nakatani T, Ozawa K, Asano M, Ukikusa M, Kamiyama Y, Tobe T. Differences in predominant energy substrate in relation to the resected hepatic mass in the phase immediately after hepatectomy. *J Lab Clin Med.* 1981; 97 (6):887–98. [PubMed: 7229515]
43. Sapiro JM, Mashek MT, Greenberg AS, Mashek DG. Hepatic triacylglycerol hydrolysis regulates peroxisome proliferator-activated receptor alpha activity. *J Lipid Res.* 2009; 50 (8):1621–9. [PubMed: 19304987]
44. Pegorier JP, Le May C, Girard J. Control of gene expression by fatty acids. *J Nutr.* 2004; 134 (9): 2444S–2449S. [PubMed: 15333740]
45. Dhe-Paganon S, Duda K, Iwamoto M, Chi YI, Shoelson SE. Crystal structure of the HNF4 alpha ligand binding domain in complex with endogenous fatty acid ligand. *J Biol Chem.* 2002; 277 (41):37973–6. [PubMed: 12193589]
46. Ou J, Tu H, Shan B, Luk A, DeBose-Boyd RA, Bashmakov Y, Goldstein JL, Brown MS. Unsaturated fatty acids inhibit transcription of the sterol regulatory element-binding protein-1c (SREBP-1c) gene by antagonizing ligand-dependent activation of the LXR. *Proc Natl Acad Sci U S A.* 2001; 98 (11):6027–32. [PubMed: 11371634]

47. Lu SC. Regulation of hepatic glutathione synthesis: current concepts and controversies. *Faseb J*. 1999; 13 (10):1169–83. [PubMed: 10385608]
48. Corrales FJ, Perez-Mato I, Sanchez Del Pino MM, Ruiz F, Castro C, Garcia-Trevijano ER, Latasa U, Martinez-Chantar ML, Martinez-Cruz A, Avila MA, Mato JM. Regulation of mammalian liver methionine adenosyltransferase. *J Nutr*. 2002; 132 (8 Suppl):2377S–2381S. [PubMed: 12163696]
49. Huang ZZ, Mao Z, Cai J, Lu SC. Changes in methionine adenosyltransferase during liver regeneration in the rat. *Am J Physiol*. 1998; 275 (1 Pt 1):G14–21. [PubMed: 9655679]
50. Martinez-Chantar ML, Vazquez-Chantada M, Garnacho M, Latasa MU, Varela-Rey M, Dotor J, Santamaria M, Martinez-Cruz LA, Parada LA, Lu SC, Mato JM. S-adenosylmethionine regulates cytoplasmic HuR via AMP-activated kinase. *Gastroenterology*. 2006; 131 (1):223–32. [PubMed: 16831604]
51. Cai J, Mao Z, Hwang JJ, Lu SC. Differential expression of methionine adenosyltransferase genes influences the rate of growth of human hepatocellular carcinoma cells. *Cancer Res*. 1998; 58 (7): 1444–50. [PubMed: 9537246]
52. Wu G, Morris SM Jr. Arginine metabolism: nitric oxide and beyond. *Biochem J*. 1998; 336 (Pt 1): 1–17. [PubMed: 9806879]
53. Lancaster JR Jr, Xie K. Tumors face NO problems? *Cancer Res*. 2006; 66 (13):6459–62. [PubMed: 16818612]
54. Fernandez V, Tapia G, Varela P, Castillo I, Mora C, Moya F, Orellana M, Videla LA. Redox up-regulated expression of rat liver manganese superoxide dismutase and Bcl-2 by thyroid hormone is associated with inhibitor of kappaB-alpha phosphorylation and nuclear factor-kappaB activation. *J Endocrinol*. 2005; 186 (3):539–47. [PubMed: 16135673]
55. Gavino VC, Dillard CJ, Tappel AL. Effect of dietary vitamin E and Santoquin on regenerating rat liver. *Life Sci*. 1985; 36 (18):1771–7. [PubMed: 2858807]
56. Aslam S, Santha T, Leone A, Wilcox C. Effects of amlodipine and valsartan on oxidative stress and plasma methylarginines in end-stage renal disease patients on hemodialysis. *Kidney Int*. 2006; 70 (12):2109–15. [PubMed: 17063175]
57. Sharma R, Yang Y, Sharma A, Awasthi S, Awasthi YC. Antioxidant role of glutathione S-transferases: protection against oxidant toxicity and regulation of stress-mediated apoptosis. *Antioxid Redox Signal*. 2004; 6 (2):289–300. [PubMed: 15025930]
58. Cairns RA, Harris IS, Mak TW. Regulation of cancer cell metabolism. *Nat Rev Cancer*. 2011; 11 (2):85–95. [PubMed: 21258394]

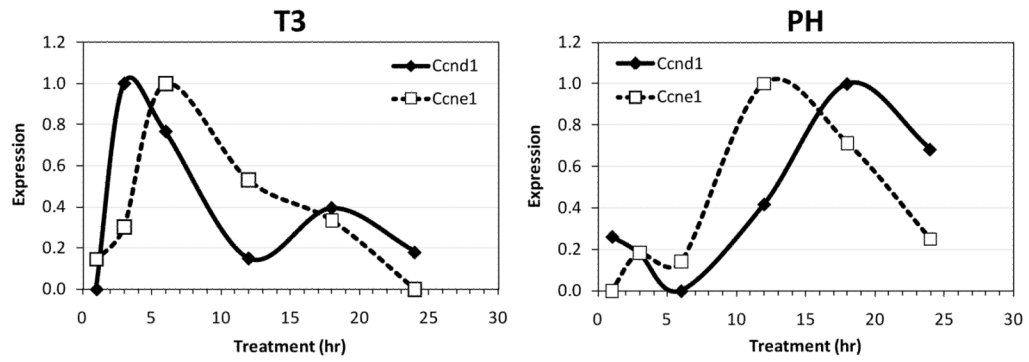


Figure 1. Expression of cell cycle regulators Cyclin D1 and E1. The plots show the patterns of change between the minimum (0) and maximum (1.0) level of expression for each mRNA. Data were averaged from 3 – 4 microarrays from each time point.

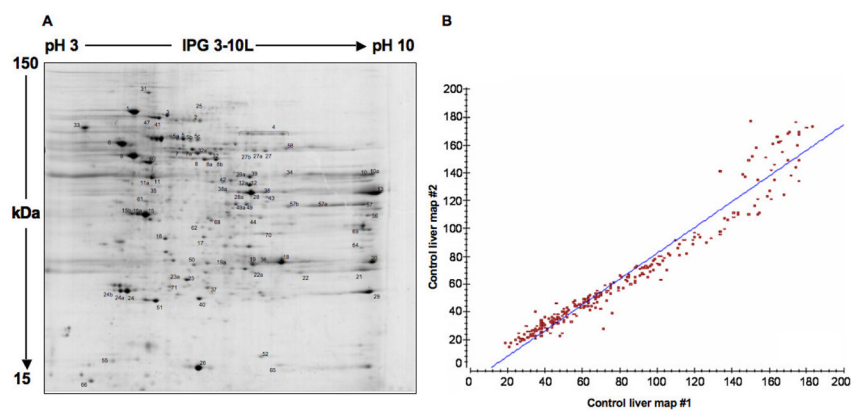


Figure 2.

A) Representative 2D-PAGE map obtained from control rat liver. 2D gel was obtained using a pH linear range of 3–10 in the first dimension and 12% SDS-PAGE in the second. Spot numbers correspond to identified proteins listed in Tables 1 and 2. B) Scatter plot of detected spots for 2D maps replicates of control samples. The high correlation coefficient (0.98) attests the good technical reproducibility.

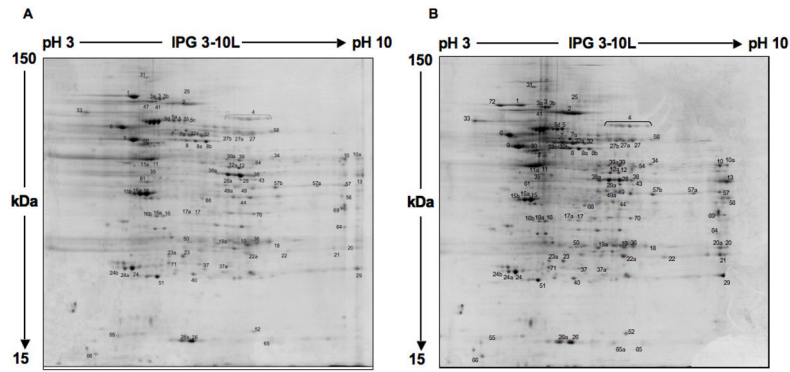


Figure 3. Representative 2D-PAGE map obtained from PH- (A) and T3-treated (B) samples. For experimental details see legend of Figure 1. Spot numbers correspond to identified proteins listed in Tables 1 and 2.

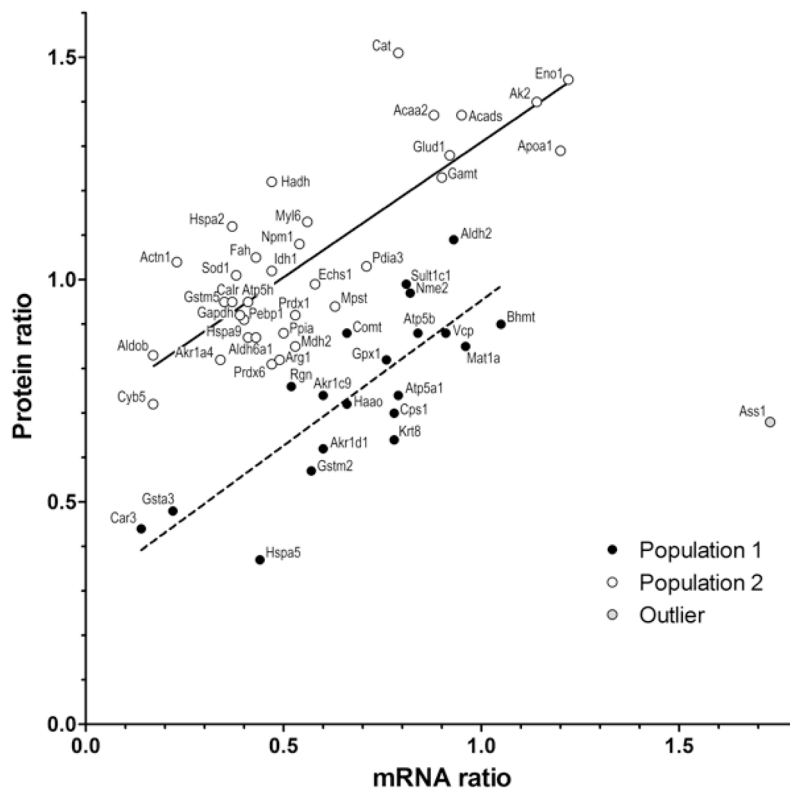


Figure 4.

Correlation of mRNA and protein levels after T3 treatment. mRNA ratios of T3-treated/control expression (x axis) were averaged from 3 two-color microarrays following cohybridization of RNA from treated and normal livers. Protein levels (y axis), also expressed as the ratio of T3-induced/ normal abundance, listed in Table 1. The plot shows the values for all proteins detected by both analyses, except serum albumin, since this high abundance serum protein varied considerably in comparable specimens. The regression analysis derives from all of the data points except Ass1 (an outlier that had increased mRNA but decreased protein). The illustrated regression analysis was optimized to reflect two populations with different RNA to protein ratios (see text).

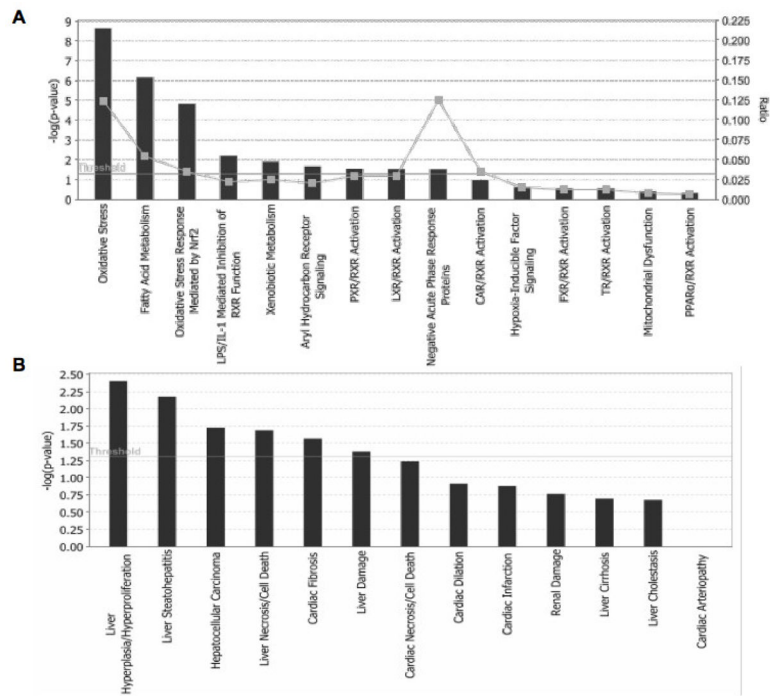


Figure 5. Significantly enriched categories of differentially expressed proteins after T3 treatment samples were classified by IPA software on the basis of biological functions (A), or tissue related pathologies classification (B).

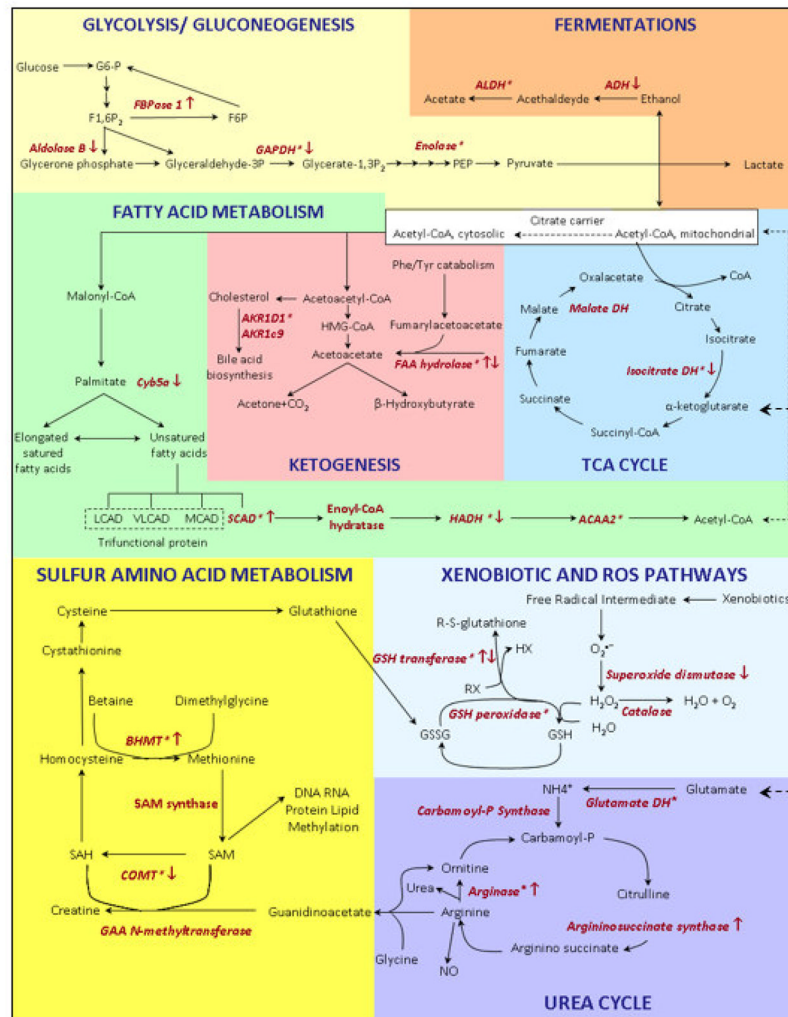


Figure 6. Overview of the metabolic pathways of differentially expressed proteins (marked in red) following T3 treatment. The regulation level is indicated by the arrows. Asterisks indicate the detection of multiple isoforms for a given enzyme. For protein annotation and fold change, see Table 1.

Differentially expressed proteins in rat liver samples following PH and T3 treatment compared to the control sample. Protein theoretical relative masses (Mr) and pI are reported along with the number of matching peptides, the coverage percentages and probability scores (Pr) for identifications. In bold are reported the significantly regulated proteins (fold change ≤ 0.5 or ≥ 1.5) in at least one condition. Spots undetected in one condition (np) are also listed.

Table 1

Spot #	Accession #	Description	Mr/pI	Coverage (%)	# Peptides	Pr. (%)	Ratio PH/Control	Ratio T3/Control
1	P06761	78 kDa glucose regulated protein (Hspa5)	72.302/4.9	57.8	44	100	0.64	0.44
2	P02770	Serum albumin precursor (Alb)	68.774/6.0	69.6	53	100	0.99	2.69
3	P48721	Stress 70 protein mitochondrial (Hspa9)	73.813/5.9	57.4	50	100	0.48	0.41
4	P04762	Catalase (Cat)	59.588/7.1	56.1	33	100	0.91	0.79
5	P11598	Protein disulfide isomerase (Pdia3)	56.587/5.8	66.3	38	99	0.49	0.71
5a	P11598	Protein disulfide isomerase (Pdia3)	56.587/5.8	66.3	38	100	0.87	np
5b	P11598	Protein disulfide isomerase (Pdia3)	56.587/5.8	66.3	38	100	0.88	np
5c	P11598	Protein disulfide isomerase (Pdia3)	56.587/5.8	66.3	38	100	0.50	np
6	P04785	Protein disulfide isomerase (P4hb)	56.915/4.6	63.3	40	100	0.72	0.70
7	Q10758	Keratin type II cytoskeletal 8 (Krt8)	53.854/5.7	61.8	28	100	0.49	0.50
7a	Q10758	Keratin type II cytoskeletal 8 (Krt8)	53.854/5.7	61.8	27	100	0.40	0.78
8	P04764	Alpha enolase (Eno1)	46.955/6.1	73	39	100	1.07	1.22
8a	P04764	Alpha enolase (Eno1)	46.955/6.1	73	39	99	0.72	0.76
8b	P04764	Alpha enolase (Eno1)	46.955/6.1	73	39	100	0.76	0.56
9	P10719	ATP synthase beta chain (Atp5b)	56.318/5.0	59.2	16	100	0.43	0.84
10	P13437	3 ketoacyl CoA thiolase (Acaa2)	41.844/7.9	82.9	35	100	0.31	0.57
10a	P13437	3 ketoacyl CoA thiolase (Acaa2)	41.844/7.9	82.9	35	98	0.30	0.66
11	O09171	Betaine homocysteine S-methyltransferase 1 (Bhmt)	44.947/7.8	79.1	36	100	0.60	1.05
11a	O09171	Betaine homocysteine S-methyltransferase 1 (Bhmt)	44.947/7.8	79.1	36	100	2.01	1.99
12	P25093	Fumarylacetoacetate hydrolase (Fah)	45.946/6.7	56.3	27	100	0.47	0.43
12a	P25093	Fumarylacetoacetate hydrolase (Fah)	45.946/6.7	56.3	27	100	1.46	2.13
13	P00884	Fructose-bisphosphate aldolase B (Aldob)	39.462/8.4	45.5	27	100	0.07	0.17
15	Q03336	Senescence marker protein 30 (Regn)	33.367/5.2	76.3	28	100	0.61	0.52
15a	Q03336	Senescence marker protein 30 (Regn)	33.367/5.2	76.3	28	100	1.48	1.22
15b	Q03336	Senescence marker protein 30 (Regn)	33.367/5.2	76.3	28	100	0.71	0.83
16	P46953	3-hydroxyanthranilate 3,4-dioxygenase (Haao)	32.561/5.5	67.1	27	87	0.58	0.66
17	P97552	3-mercaptopyruvate sulfurtransferase (Mpst)	32.788/5.8	44.6	15	100	0.46	0.63

Spot #	Accession #	Description	Mr/pI	Coverage (%)	# Peptides	Pr. (%)	Ratio PH/ Control	Ratio T3/ Control
18	P14141	Carbonic anhydrase III (Ca3)	29.281/7.0	83	18	100	0.23	0.14
19	P14604	Enoyl CoA hydratase (Echs1)	31.496/8.2	56.6	25	100	0.70	0.58
19a	P14604	Enoyl CoA hydratase (Echs1)	31.496/8.2	56.6	25	84	0.56	0.54
20	P04904	Glutathione S transferase Yc 1 (Gsta3)	25.172/9.1	47.7	16	100	0.33	0.22
21	P04905	Glutathione S transferase Yb1 (Gstm1)	25.766/8.4	75.1	22	100	0.28	0.35
22	P08010	Glutathione S transferase Yb2 (Gstm2)	25.554/7.2	94.5	38	100	0.37	0.57
22a	P08010	Glutathione S transferase Yb2 (Gstm2)	25.554/7.2	94.5	38	100	1.25	2.29
23	O35244	Antioxidant protein 2 (Prdx6)	24.671/5.5	87.4	27	99	0.49	0.47
23a	O35244	Antioxidant protein 2 (Prdx6)	24.671/5.5	87.4	27	100	0.91	0.90
24	P22734	Catechol O methyltransferase (Comt)	29.578/5.3	51.1	17	100	0.62	0.66
24a	P22734	Catechol O methyltransferase (Comt)	29.578/5.3	51.1	17	100	0.54	0.52
24b	P22734	Catechol O methyltransferase (Comt)	29.578/5.3	51.1	17	100	0.65	0.20
25	P07756	Carbamoyl-phosphate synthase (Cps1)	164.474/6.3	38.8	72	100	0.38	0.78
26	P07632	Superoxide dismutase (Sod1)	15.770/5.9	53.6	11	100	0.55	0.38
27	P10860	Glutamate dehydrogenase (Glud1)	61.389/8.0	49.1	32	100	0.47	0.92
27a	P10860	Glutamate dehydrogenase (Glud1)	61.389/8.0	49.1	32	99	0.31	0.76
27b	P10860	Glutamate dehydrogenase (Glud1)	61.389/8.0	49.1	32	100	0.57	1.16
28	P07824	Arginase 1 liver type (Arg1)	34.951/6.9	71.8	24	100	0.66	0.49
28a	P07824	Arginase 1 liver type (Arg1)	34.951/6.9	71.8	24	100	2.67	3.41
29	Q63716	Peroxisome oxidin 1 (Prdx1)	22.095/8.2	55.8	16	98	0.18	0.53
31	P46462	Transitional endopl ret ATPase (Vcp)	89.292/4.9	47	48	100	0.58	0.91
32	P11884	Aldehyde dehydrogenase, mitochondrial (Aldh2)	56.452/6.7	52.8	35	100	1.16	0.93
32a	P11884	Aldehyde dehydrogenase, mitochondrial (Aldh2)	56.452/6.7	52.8	35	100	0.63	0.99
33	P18418	Calreticulin (Calr)	47.965/4.1	51	24	100	0.48	0.37
34	P09034	Argininosuccinate synthase (Ass1)	46.466/7.7	51.7	25	100	0.32	1.73
35	P19112	Fructose 1, 6 biphosphatase (Fbp1)	39.453/5.4	42.8	14	100	0.89	1.69
36	P29410	Adenylate kinase (Akd2)	26.231/6.3	66.4	18	100	1.04	1.14
37	P04041	Glutathione peroxidase (Gpx1)	22.244/7.8	69.7	16	100	0.81	0.76
38	P15651	Acyl CoA dehydrogenase (Acads)	44.736/8.4	48.3	21	87	0.84	0.95
38a	P15651	Acyl CoA dehydrogenase (Acads)	44.736/8.4	48.3	21	100	0.65	2.63
39	P41562	Isocitrate dehydrogenase [NADP] (Idh1)	46.704/6.6	65.9	41	100	0.38	0.47

Spot #	Accession #	Description	Mr/pI	Coverage (%)	# Peptides	Pr. (%)	Ratio PH/ Control	Ratio T3/ Control
39a	P41562	Isocitrate dehydrogenase [NADP] (Idh1)	46.704/6.6	65.9	41	100	0.70	1.13
40	P31399	ATP synthase D chain (Atp5h)	18.620/6.2	77.5	16	84	0.50	0.41
41	P14659	Heat shock related 70 kDa (Hspa2)	69.485/5.3	49.1	26	100	0.18	0.37
43	P51635	Alcohol dehydrogenase [NADP+] (Akr1a1)	36.351/7.0	46.3	16	100	0.72	0.34
44	P23457	3-alpha-hydroxysteroid dehydrogenase (Akr1c9)	37.003/6.7	42.9	10	100	1.63	0.60
47	Q07439	Heat shock 70 kDa (Hspa1b)	70.120/5.3	41.9	26	100	0.43	np
49	P31210	3-oxo-5 beta steroid 4 dehydrogenase (Akr1d1)	37.354/6.2	52.1	20	99	0.26	0.60
49a	P31210	3-oxo-5 beta steroid 4 dehydrogenase (Akr1d1)	37.354/6.2	52.1	20	100	0.33	0.64
50	P10868	Guanidinoacetate (GAA) N-methyltransferase (Gamt)	26.259/5.6	74.5	20	100	0.95	0.90
51	P31044	Phosphatidylethanol binding protein (Pebp1)	20.788/5.4	72.2	10	100	0.61	0.40
52	P19804	Nucleoside diphosphate kinase B (Nme2)	17.271/7.3	84.9	15	100	0.75	0.82
55	P00173	Cytochrome B5 (Cyb5a)	15.214/4.7	41.4	4	100	1.15	0.17
56	P04636	Malate dehydrogenase (Mdh2)	35.632/8.8	69.2	31	100	0.47	0.53
57	P04797	Glyceraldehyde-3-phosphate dehydrogenase (Gapdh)	35.682/8.3	48.8	15	100	0.21	0.39
57a	P04797	Glyceraldehyde-3-phosphate dehydrogenase (Gapdh)	35.682/8.3	48.8	15	99	0.21	0.66
57b	P04797	Glyceraldehyde-3-phosphate dehydrogenase (Gapdh)	35.682/8.3	48.8	15	100	0.75	0.93
58	Q02253	Malonate-semialdehyde dehydrogenase (Aldh6a1)	57.770/8.2	61.9	33	100	0.45	0.43
60	Q9Z1P2	Alpha actinin 1 (Actn1)	102.895/5.1	36.9	32	100	0.18	0.23
61	P13444	S-adenosylmethionine (SAM) synthetase (Mata1)	43.670/5.5	48.9	18	98	1.19	0.96
64	P15999	ATP synthase A chain (Atp5a1)	58.790/9.5	54.7	28	100	0.57	0.79
65	P10111	Peptidyl prolyl cis trans isomerase (Ppia)	17.731/8.3	84	16	100	1.04	0.50
66	Q64119	Myosin light chain (Myl6)	16.833/4.3	56	10	83	0.43	0.56
68	P50237	Sulfotransferase 1C1 (Sult1c1)	35.740/6.1	52.5	13	84	0.75	0.81
69	Q9WVK7	Hydroxyacyl-coenzyme A dehydrogenase (Hadh)	34.425/9.2	71.5	16	100	0.40	0.47
70	P13084	Nucleophosmin (Npm1)	32.539/4.4	43.8	14	81	0.89	0.54
71	P04639	Apolipoprotein A1 (Apoa1)	30.069/5.4	67.6	31	100	0.83	1.20

Table 2

Protein spots uniquely revealed under a given analysed conditions. See Table 1 for heading details.

Spot #	Accession #	Description	Mr/pI	Coverage (%)	# Peptides	Pr. (%)	Condition
3a	P48721	Stress 70 protein mitochondrial (Hspa9)	73.813/5.9	57.4	50	100	PH/T3
3b	P48721	Stress 70 protein mitochondrial (Hspa9)	73.813/5.9	57.4	50	100	PH/T3
5d	P11598	Protein disulfide isomerase (Pdia3)	56.587/5.8	66.3	38	100	T3
16a	P46953	3-hydroxyanthranilate 3,4-dioxygenase (Haao)	32.561/5.5	67.1	27	100	PH/T3
16b	P46953	3-hydroxyanthranilate 3,4-dioxygenase (Haao)	32.561/5.5	67.1	27	100	PH/T3
17a	P97532	3-mercaptopyruvate sulfurtransferase (Mpst)	32.788/5.8	44.6	15	99	PH/T3
20a	P04904	Glutathione S transferase γ c 1 (Gsta3)	25.172/9.1	47.7	16	100	T3
26a	P07632	Superoxide dismutase (Sod1)	15.770/5.9	53.6	11	100	PH/T3
32b	P11884	Aldehyde dehydrogenase (Aldh2)	56.452/6.7	52.8	35	100	T3
32c	P11884	Aldehyde dehydrogenase (Aldh2)	56.452/6.7	52.8	35	100	T3
37a	P04041	Glutathione peroxidase (Gpx1)	22.244/7.8	69.7	16	100	PH/T3
54	P16617	Phosphoglycerate kinase (Pkg1)	44.394/7.6	44.2	19	87	PH/T3
65a	P10111	Peptidyl prolyl cis trans isomerase (Ppia)	17.731/8.3	84	16	100	PH/T3
42	Q03248	Beta ureidopropionase (Ubp1)	44.013/6.5	53.7	25	100	Control
62	P14669	Annexin III - Lipocortin III (Anxa3)	36.299/6.0	54.6	17	84	Control

Table 3

Relative mRNA levels after T3 treatment. Ratios were calculated from dual hybridization of RNA livers 6 hr after T3 treatment / untreated control liver. The data were averaged from three arrays.

Description	Ratio T3/ Control	SD
Catalase (Cat)	1.51	1.11
Alpha enolase (Eno1)	1.45	0.24
Adenylate kinase (Ak2)	1.40	0.19
Acyl CoA dehydrogenase (Acads)	1.37	0.26
3 ketoacyl CoA thiolase (Acaa2)	1.37	0.58
Apolipoprotein A1 (Apoa1)	1.29	0.24
Glutamate dehydrogenase (Glud1)	1.28	0.06
Guanidinoacetate (GAA) N-methyltransferase (Gamt)	1.23	0.32
Hydroxyacyl-coenzyme A dehydrogenase (Hadh)	1.22	0.41
Myosin light chain (Myl6)	1.13	0.21
Heat shock related 70 kDa (Hspa2)	1.12	0.01
Aldehyde dehydrogenase, mitochondrial (Aldh2)	1.09	0.64
Nucleophosmin (Npm1)	1.08	0.11
Fumarylacetoacetate hydrolase (Fah)	1.05	0.27
Alpha actinin 1 (Actn1)	1.04	0.25
Protein disulfide isomerase 3 (Pdia3)	1.03	0.15
Fructose 1, 6 bisphosphatase (Fbp1)	1.02	0.08
Isocitrate dehydrogenase [NADP] (Idh1)	1.02	0.15
Superoxide dismutase (Sod1)	1.01	0.10
Sulfotransferase 1C1 (Sult1c1)	0.99	0.08
Enoyl CoA hydratase (Echs1)	0.99	0.14
Nucleoside diphosphate kinase B (Nme2)	0.97	0.31
Glutathione S transferase Yb1 (Gstm1)	0.95	0.15
Serum albumin precursor (Alb)	0.95	0.15
ATP synthase D chain (Atp5h)	0.95	0.45
Calreticulin (Calr)	0.95	0.22
3-mercaptopyruvate sulfurtransferase (Mpst)	0.94	0.22
Peroxisome oxidin 1 (Prdx1)	0.92	0.28
Glyceraldehyde-3-phosphate dehydrogenase (Gapdh)	1.12	0.26
Phosphatidylethanol binding protein (Pepb1)	0.91	0.40
Betaine homocysteine S-methyltransferase 1 (Bhmt)	0.90	0.43
Peptidyl prolyl cis trans isomerase (Ppia)	0.96	0.32
ATP synthase beta chain (Atp5b)	0.88	0.18
Catechol O methyltransferase (Comt)	0.88	0.12
Transitional endopl ret ATPase (Vcp)	0.88	0.13
Malonate-semialdehyde dehydrogenase (Aldh6a1)	0.87	0.10

Description	Ratio T3/ Control	SD
Stress 70 protein mitochondrial (Hspa9)	0.87	0.14
S-adenosylmethionine (SAM) synthetase (Mata1)	0.85	0.16
Malate dehydrogenase (Mdh2)	0.85	0.14
Fructose-bisphosphate aldolase B (Aldob)	0.83	0.09
Alcohol dehydrogenase [NADP+] (Akr1a1)	0.82	0.22
Glutathione peroxidase (Gpx1)	0.82	0.06
Arginase 1 liver type (Arg1)	0.82	0.39
Antioxidant protein 2 (Prdx6)	0.81	0.08
Senescence marker protein 30 (Regn)	0.76	0.15
ATP synthase A chain (Atp5a1)	0.74	0.04
3-alpha-hydroxysteroid dehydrogenase (Akr1c9)	0.74	0.11
Cytochrome B5 (Cyb5a)	0.72	0.08
3-hydroxyanthranilate 3,4-dioxygenase (Haa0)	0.72	0.20
Carbamoyl-phosphate synthase (Cps1)	0.70	0.43
Argininosuccinate synthase (Ass1)	0.68	0.32
Keratin type II cytoskeletal 8 (Krt8)	0.64	0.13
3-oxo-5-beta-steroid 4-dehydrogenase (Akr1d1)	0.62	0.13
Glutathione S transferase Yb2 (Gstm2)	0.57	0.19
Glutathione S transferase Yc 1 (Gsta3)	0.48	0.08
Carbonic anhydrase III (Ca3)	0.44	0.14
78 kDa glucose regulated protein (Hspa5)	0.37	0.07

Table 4

mRNA levels of genes related to lipid metabolism. Ratios were calculated as in Table 3.

Description	Ratio T3/Control	SD
Carnitine palmitoyltransferase 1a liver (Cpt1a)	2.34	0.91
Patatin-like phospholipase domain containing 2 (Pnpla2)	2.26	0.99
Apolipoprotein A-IV (Apoa4)	1.95	1.15
Dodecenoyl-Coenzyme A delta isomerase (3 2 trans-enoyl-Coenzyme A isomerase; Dci)	1.83	0.86
Carnitine acetyltransferase (Crat)	1.81	0.43
Adipose differentiation related protein (Adfp)	1.75	0.53
Peroxisomal acyl-CoA thioesterase 2B (Pte2b)	1.66	0.63
Cytochrome P450 4a14 (Cyp4a14)	1.62	0.60
Sphingosine phosphate lyase 1 (Sgp11)	1.49	0.58
Lysophospholipase 2 (Lypla2)	1.48	0.23
Low-density lipoprotein receptor-related protein 10 (Lrp10)	1.42	0.46
Monoglyceride lipase (Mgl1)	1.39	0.07
Lipocalin 10 (Lcn10)	0.67	0.18
Glycerophosphodiester phosphodiesterase domain containing 5 (Gdpd5)	0.66	0.33
Acyl-CoA wax alcohol acyltransferase 2 (Awat2)	0.58	0.18
Lipin 2 (Lpin2)	0.58	0.10
Phosphatidylglycerophosphate synthase 1 (Pgs1)	0.58	0.12
Apolipoprotein B (Apob)	0.51	0.19
STAR-related lipid transfer (START) domain containing 6 (Stard6)	0.47	0.25
DDHD domain containing 2 (Ddhd2)	0.44	0.10
Lipase, member I (Lipi)	0.42	0.11
Propionyl coenzyme A carboxylase beta polypeptide (Pccb)	0.30	0.04
Lipase-like abhydrolase domain containing 3 (Lipl3)	0.24	0.04